Submitted to

XV International Workshop on Deep-Inelastic Scattering and Related Subjects,
DIS 2007 April 16-20, 2007, Munich

www-h1.desy.de/h1/www/publications/conf/conf_list.html

A search for excited electrons at HERA

H1 Collaboration

Abstract

We present a search for excited electrons using all data collected by the H1 experiment at HERA at a center-of-mass energy of 320 GeV with an integrated luminosity of 435 pb^{-1}. The electroweak decay of excited electrons, $e^* \to e\gamma$, $e^* \to eZ$, $e^* \to \nu W$ are considered and possible final states resulting from the Z or W hadronic decays are taken into account. No evidence for excited electron production is found. Mass dependent exclusion limits are determined for the ratio of the coupling to the compositeness scale, f/Λ. These limits extend the excluded region to higher masses than has been possible in previous searches.

1 Introduction

The discovery of excited states of quarks or leptons as predicted by compositness models [1, 2] would provide a convincing evidence for a new substructure of matter. Electron[1]-proton interactions at very high energies provide an excellent environement to look for excited states of first generation fermions. In particular, these excited electrons (e^*) could be singly produced throught t-channel γ or Z boson exchange.

In this paper we present a search for excited electrons using all HERA collider data of the H1 experiment. The data collected at electron and proton beam energies of 27.6 GeV and 920 GeV respectively corresponds to an integrated luminosity of 435 pb^{-1}. The excited electrons are searched for through all their electroweak decays into a fermion and a gauge boson (γ, W and Z). Only hadronic decays of the W and Z bosons are considered.

2 Phenomenology

Compositeness models [1–4] attempt to explain the hierarchy of masses in the Standard Model by the existence of a substructure within the fermions. Several of these models predict excited states of the known leptons. Excited leptons are assumed to have the same electroweak SU(2) and U(1) gauge couplings, g and g', to the vector bosons, but are expected to be grouped into both left- and right-handed weak isodoublets with vector couplings. The existence of the right-handed doublets is required.

In ep collisions, excited leptons could be produced via the process $ep \to F^* X$ (here X represents the proton remnant or proton in the case of elastic e^* production), as a result of the F*FV couplings. Depending on the details of these couplings, excited leptons could be detected in the photonic, charged current, or neutral current channels.

The branching ratio of the excited leptons into the different vector bosons are determined by the strength of the three F*FV couplings. We use the effective Lagrangian:

$$L_{F^*F} = \frac{1}{2\Lambda}\bar{F}^*_R \sigma^{\mu\nu}[g f \frac{\vec{\tau}}{2}\partial_\mu \vec{W}_\nu + g' f' \frac{Y}{2}\partial_\mu B_\nu]F_L + h.c. \quad (1)$$

which describes the generalised magnetic de-excitation of the excited states. The matrix $\sigma^{\mu\nu}$ is the covariant bilinear tensor, τ are the Pauli matrices, $W_{\mu\nu}$ and $B_{\mu\nu}$ represent the fully gauge invariant field tensors, and Y is the weak hypercharge. The parameter Λ has units of energy and can be regarded as the compositeness scale, while f and f' are the weight associated with the different gauge groups.

The relative values of f and f' also affect the size of the single-production cross-sections and their detection efficiencies. Depending on their relative values, either the photonic decay, the CC decay, or the NC decay will have the largest branching ratio, depending on the respective couplings:

$$f_\gamma = e_f f' + I_{3L}(f - f'), f_W = \frac{f}{\sqrt{2}s_\omega}, f_Z = \frac{4I_{3L}(c^2_\omega f + s^2_\omega f') - 4e_f s^2_\omega f'}{4 s_\omega c_\omega}$$

[1] the term "electron" is used generically to refer to both electrons and positrons.

where e_f is the excited fermion charge, I_{3L} is the weak isospin, and $s_\omega(c_\omega)$ are the sine (cosine) of the Weinberg angle θ_ω.

The following results for excited electrons will be interpreted using the conventional coupling assignments, $f = +f'$.

3 Standard Model processes and their simulation

Final states of events selection in this analysis contain either missing transverse momentum or an high energy electron (or photon) and a photon or jets with high tranverse energy. The main backgrounds from Standard Model (SM) processes which could mimic such signatures are mostly neutral current (NC) and charged current (CC) deep-inelastic scattering (DIS) or photoproduction processes. The Born, QCD Compton and Boson Gluon Fusion matrix elements are used in the RAPGAP [5] event generator to model NC DIS and CC DIS events. The QED radiative effects arising from real photon emission from both the incoming and outgoing electrons are simulated using the HERACLES [7] generator. To simulate the direct and resolved photoproduction of jets, prompt photon production and the resolved photoproduction of photon pairs, the PYTHIA 6.1 event generator [6] is used. Light and heavy flavoured jets are generated. The simulation contains the Born level hard scattering matrix elements and radiative QED corrections. Processes with the production of three or more jets are accounted for using leading logarithmic parton showers as a representation of higher order QCD radiation. Hadronisation is modelled using Lund string fragmentation [6]. The prediction of processes with two or more high transverse momentum jets is scaled by a factor of 1.2 to normalise the leading order Monte Carlos to next-to-leading order QCD calculations [8]. Contributions from elastic and quasi-elastic QED-Compton scattering are simulated with the WABGEN [9] generator. Possible contributions arising from the production of W bosons or multi-lepton events are also considered and modelled using the EPVEC [10] and GRAPE [11] event generators, respectively.

All generated events are passed through the full GEANT [12] based simulation of the H1 apparatus, which takes into account the running conditions of the different data taking periods.

4 The H1 Detector

A detailed description of the H1 experiment can be found in [13]. Only the H1 detector components relevant to the present analysis are briefly described here. Jets and electrons are measured with the Liquid Argon (LAr) calorimeter [14], which covers the polar angle[2] range $4^\circ < \theta < 154^\circ$ with full azimuthal acceptance. Electromagnetic shower energies are measured with a precision of $\sigma(E)/E = 12\%/\sqrt{E/\text{GeV}} \oplus 1\%$ and hadronic energies with $\sigma(E)/E = 50\%/\sqrt{E/\text{GeV}} \oplus 2\%$, as measured in test beams. In the backward region, energy

[2]The origin of the H1 coordinate system is the nominal ep interaction point, with the direction of the proton beam defining the positive z-axis (forward region). The transverse momenta are measured in the xy plane. The pseudorapidity η is related to the polar angle θ by $\eta = -\ln\tan(\theta/2)$.

measurements are provided by a lead/scintillating-fiber (SpaCal) calorimeter [15] covering the range $155^\circ < \theta < 178^\circ$. The central and forward tracking detectors are used to measure charged particle trajectories, to reconstruct the interaction vertex and to supplement the measurement of the hadronic energy. The LAr and inner tracking detectors are enclosed in a super-conducting magnetic coil with a strength of 1.15 T. The luminosity measurement is based on the Bethe-Heitler process $ep \to ep\gamma$, where the photon is detected in a calorimeter located downstream of the interaction point.

5 Data Analysis

Events are first selected by requiring that the event vertex be reconstructed within 35 cm in z of the nominal interaction point. In addition topological filters and timing vetoes are applied to remove background events induced by cosmic showers and other non-ep sources. The main trigger of the events is provided by the LAr calorimeter. The trigger efficiency is close to 100% for events having an electromagnetic deposit in the LAr (electron or photon) with an energy greater than 10 GeV [16]. For events with missing transverse momentum above 20 GeV, the trigger efficiency is ~ 90 %.

The identification of electrons or photons is first based on the measurement of a compact and isolated electromagnetic shower in the LAr calorimeter. In addition, the electromagnetic cluster is required to be be isolated from jets by a distance $R > 0.5$ to the jet axis in pseudorapidity-azimuth. Energy deposits in the calorimeter and tracks in the inner tracking system are used to form combined cluster-track objects, from which the hadronic energy is reconstructed. Jets are defined using an inclusive k_T algorithm [17, 18] with a minimum transverse momentum of 3 GeV. The missing transverse momentum P_T^{miss} of the event is derived from all identified particles and energy deposits in the event.

5.1 $e\gamma$ Resonance Search

The signature of this channel consist of two isolated electromagnetic cluster with an high transverse momentum. The principal SM background arise from elastic and inelastic Compton events. Two isolated electromagnetic clusters in the polar angle $5^\circ < \theta_{e1,e2} < 130^\circ$ are first required, with a transverse momentum larger than 20 and 15 GeV, respectively. To further suppress contributions from Compton events, the sum of the energies of the two electromagnetic clusters has to be greater than 100 GeV and the sum of their total transverse momentum should be larger than 75 GeV. Finally, 112 events survives the selection criteria. The expected SM contribution is 125 ± 19 events and is dominated by Compton events. The resulting selection efficiency varies from 60% to 70% for excited electrons of mass 100 GeV and 250 GeV, respectively.

5.2 $\nu q\bar{q}$ Resonance Search

For this search, the dominant SM background consists of multi-jet CC DIS events with a moderate contribution from photoproduction. The presence of a neutrino is inferred from substantial

missing momentum $P_T^{miss} > 20$ GeV. We use a subsample of events with at least two jets, each having a transverse momentum larger than 20 and 15 GeV, respectively, and a polar angle between $5°$ and $130°$. The ratio V_{ap}/V_p of transverse energy flow anti-parallel and parallel to the hadronic final state [16] is used to suppress photoproduction events. Events with $V_{ap}/V_p > 0.3$ are rejected. The W candidate is reconstructed from the combination of two jets with an invariant mass closest to the nominal W boson mass. The reconstructed mass is required to be above 50 GeV and above 65 GeV for events whose missing energy E^{miss} is below 65 GeV. After these cuts, 172 events are found compared to an expected SM contribution of 175 ± 39 events. No significant excess is observed. The acceptance for e^* events in this final state is approximately 40 % for $M_{e^*} > 150$ GeV.

5.3 e$q\bar{q}$ Resonance Search

In this channel multi-jet NC DIS events constitute the main contribution from SM processes. Events are selected by the presence of an electron in the LAr ($5° < \theta^e < 130°$) with $Q_e^2 > 2500$ GeV^2 or a tranverse momentum P_T^e greater than 25 GeV. The restriction on the electron polar angle to the forward region of the LAr removes a large part of the NC DIS contribution. The presence of at least two high P_T jets with $P_T^{jet1,\,jet2} > 20, 15$ GeV and $5° < \theta^{jet1,\,jet2} < 130°$ is required. Then, a Z candidate is reconstructed in those events from the combination of two jets with an invariant mass closest to the nominal Z boson mass. The reconstructed mass of the Z candidate M_{jj} is required to be larger than 61 GeV. To increase the separation power between NC DIS events and a ν^* signal we demand that the polar angle of the highest P_T jet associated to the Z candidate be lower than $80°$ and that $M_{jj} > 76$ GeV for the events with $P_T^e < 65$ GeV. After the selection, 351 events are observed while 318 ± 64 are expected from the SM background. The efficiency for selecting e^* events is of the order of 45 % in this decay channel.

6 Interpretation

The event yields observed in each decay channel are summarised in table 1. The observed event yields are in good agreement with SM expectations, which are dominated by NC DIS for $eq\bar{q}$ resonance search, by CC DIS events in the $\nu q\bar{q}$ decay cahnenl, and by Compton events for the $e\gamma$ resonance search. The distributions of the invariant mass of the data events and of expected SM background are compared in figure 1 for the three channels. Both data and SM are in good agreement and no additional resonance is seen in the data. No data events is observed in channels corresponding to leptonic decays of W or Z bosons in agreement with SM expectations below one in those classes.

Since there is no evidence for excited electrons, an upper limit on the coupling f/Λ as a function of the mass of the excited electron is derived. The limit is presented at the 95 % confidence level and is obtained using a modified frequentist approach [19] which takes statistical and systematical uncertainties into account.

The resulting limit after combination of the three decay channels is presented in figure 2, for the conventional assumptions $f = +f'$. This new result improve significantly the bounds

previously obtained by H1 [20] using 120 pb^{-1} of HERA I data. Considering the assumption $f/\Lambda = 1/M_{e^*}$ excited electrons with masses up to 273 GeV are excluded.

For comparisons, combined direct and indirect limits obtained in e^+e^- collisions at LEP are also shown on figure 2, as well as the result from the CDF experiment [21] at the Tevatron. The limits from the present analysis are more stringent at high masses and extend beyond the kinematic reach of previous searches.

7 Summary

In summary, using all data collected by the H1 experiment at a center-of-mass energy of 320 GeV with an integrated luminosity of 435 pb^{-1} a search for the production of excited electrons has been performed. The excited electron decay channels $e^*\to e\gamma$, $e^*\to eZ$ and $e^*\to \nu W$ with subsequent hadronic decays of the W and Z bosons have been considered and no indication of a signal was found. New limits on the coupling f/Λ as a function of the excited electron masses have been established, using the specific relation between the couplings $f = +f'$. Assuming $f = +f'$ and $f/\Lambda = 1/M_{e^*}$ excited electrons with a mass lower than 273 GeV are excluded at 95% confidence level. The present results greatly extend previous searched domains at HERA and is complementary to searches for excited electrons performed at other colliders.

References

[1] H. Harari, Phys. Rept. **104** (1984) 159.

[2] F. Boudjema, A. Djouadi and J. L. Kneur, Z. Phys. C **57** (1993) 425.

[3] K. Hagiwara, D. Zeppenfeld and S. Komamiya, Z. Phys. C **29** (1985) 115.

[4] U. Baur, M. Spira and P. M. Zerwas, Phys. Rev. D **42** (1990) 815.

[5] H. Jung, Comput. Phys. Commun. **86** (1995) 147.

[6] T. Sjostrand, P. Eden, C. Friberg, L. Lonnblad, G. Miu, S. Mrenna and E. Norrbin, Comput. Phys. Commun. **135** (2001) 238, [hep-ph/0010017].

[7] A. Kwiatkowski, H. Spiesberger and H. J. Mohring, Comput. Phys. Commun. **69** (1992) 155.

[8] C. Adloff *et al.* [H1 Collaboration], Eur. Phys. J. C **25** (2002) 13, [hep-ex/0201006].

[9] C. Berger and P. Kandel, Prepared for Workshop on Monte Carlo Generators for HERA Physics Hamburg, Germany, 27-30 Apr 1998.

[10] U. Baur, J. A. Vermaseren and D. Zeppenfeld, Nucl. Phys. B **375** (1992) 3.

[11] T. Abe, Comput. Phys. Commun. **136** (2001) 126, [hep-ph/0012029].

[12] R. Brun, F. Bruyant, M. Maire, A. C. McPherson and P. Zanarini, CERN-DD/EE/84-1.

[13] I. Abt *et al.* [H1 Collaboration], Nucl. Instrum. Meth. A **386** (1997) 310 and 348.

[14] B. Andrieu *et al.* [H1 Calorimeter Group Collaboration], Nucl. Instrum. Meth. A **336** (1993) 460.

[15] R. D. Appuhn *et al.* [H1 SPACAL Group Collaboration], Nucl. Instrum. Meth. A **386** (1997) 397.

[16] C. Adloff *et al.* [H1 Collaboration], Eur. Phys. J. C **30**, 1 (2003), [hep-ex/0304003].

[17] S. D. Ellis and D. E. Soper, Phys. Rev. D **48** (1993) 3160 [hep-ph/9305266].

[18] S. Catani, Y. L. Dokshitzer, M. H. Seymour and B. R. Webber, Nucl. Phys. B **406** (1993) 187.

[19] T. Junk, Nucl. Instrum. Meth. A **434** (1999) 435, [hep-ex/9902006].

[20] C. Adloff *et al.* [H1 Collaboration], Phys. Lett. B **548** (2002) 35 [arXiv:hep-ex/0207038].

[21] D. Acosta *et al.* [CDF Collaboration], Phys. Rev. Lett. **94** (2005) 101802, [hep-ex/0410013].

Search for e* HERA I+II ($\sqrt{s} = 320$ GeV, 435 pb^{-1}, preliminary)

Selection	Data	SM	Efficiency $\times$ BR
$e^* \to \nu W_{\hookrightarrow qq}$	172	175 ± 39	~ 40 %
$e^* \to e Z_{\hookrightarrow qq}$	351	318 ± 64	~ 45 %
$e^* \to e\gamma$	112	125 ± 19	60–70 %

Table 1: Observed and predicted event yields for the studied decay channels. The analysed data sample corresponds to an integrated luminosity of 435 pb^{-1}. The errors on the prediction include model uncertainties and experimental systematic errors added in quadrature.

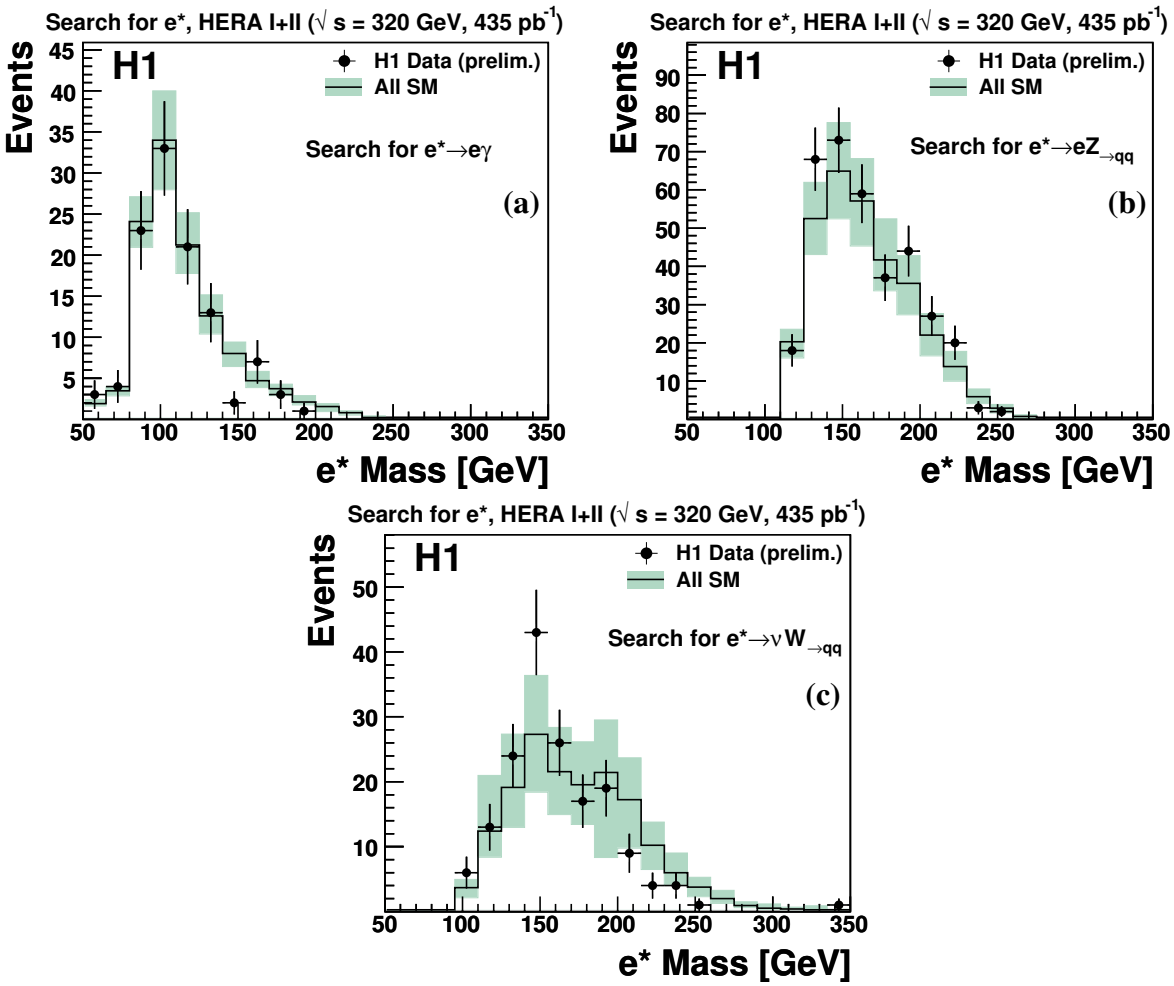

Figure 1: Invariant mass distribution of the e^* candidates for the (a) $e^* \to e\gamma$, (b) $e^* \to e Z_{\hookrightarrow q\bar{q}}$ and (c) $e^* \to \nu W_{\hookrightarrow q\bar{q}}$ searches. The points corresponds to the observed data events in the final selections and the histogram to the total SM prediction. The error bands on the SM prediction include model uncertainties and experimental systematic errors added in quadrature.

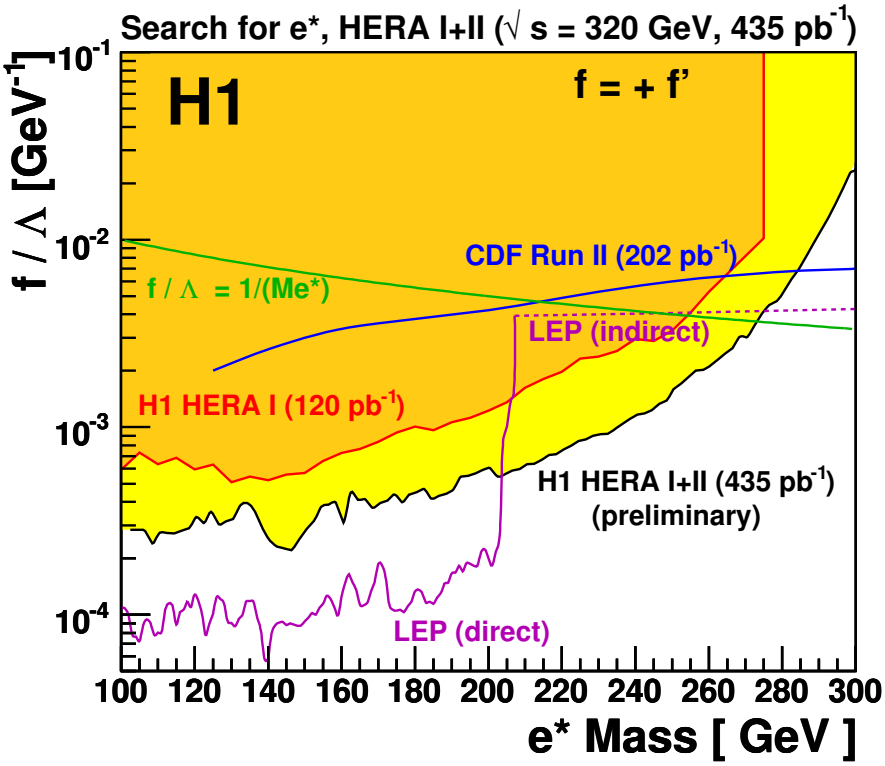

Figure 2: Exclusion limits on the coupling f/Λ at 95% C.L. as a function of the mass of the excited electron with the assumption $f = +f'$. The observed limits from this analysis using 435 pb^{-1} of H1 data is represented by the yellow area. Values of the couplings above the curves are excluded. The orange-dark area corresponds to the exclusion domain published by the H1 experiment [20] using HERA I data. The combined exclusion limit from LEP experiments is represented by the violet line, for direct (plain line) and indirect searches (dashed line) for excited electrons. The result from the CDF experiment [21] are also shown (blue line).